ChemPubSoc Europe

DOI: 10.1002/chem.201502798

CHEMISTRY A European Journal Full Paper

Synthetic Methods

Synthesis, Properties, and Two-Dimensional Adsorption Characteristics of 5-Amino[6]hexahelicene

Maarten W. van der Meijden,[a] Edith Gelens,[b] Natalia Murillo Quirós,[c, d] Javier D. Fuhr,[c] J. Esteban Gayone,[c] Hugo Ascolani,[c] Klaus Wurst,[e] Magalí Lingenfelder,*[f] and Richard M. Kellogg*[a]

Abstract: A convergent synthesis of racemic 5-amino[6]hexahelicene is described. Cross-coupling reactions are used to assemble a pentacyclic framework, and a metal-catalyzed ring-closure comprises the final step. The enantiomers were separated by means of chromatography and the absolute configurations were assigned by comparison of the CD spectra with hexahelicene. The $t_{1/2}$ value for racemization at 210 °C was approximately 1 hour. Scanning tunneling microscopy (STM) measurements were carried out on enantiopure and racemic samples of aminohelicene on Au(111) under ultrahigh vacuum (UHV) conditions.

Introduction

Helicenes, *ortho*-fused polycyclic aromatic or heteroaromatic compounds, are prime examples of molecules with axial chirality and, with regard to electronic transitions, are inherently chiral chromophores.[1] Steric interactions force nonplanarity on the aromatic system. This nonplanarity results in right-or left-handed *P*- and *M*-helices, respectively, the enantiomeric stability of which depends on the amount of steric interaction, which usually increases with the number of rings. Sufficient stability to enantiomerization to allow the possibility of isolation generally commences at a length of five fused rings. Owing to their unusual and highly interesting electronic and optical properties, helicenes could lend themselves for use in electronic devices.[2] With a facile synthesis in hand, it should be possible to examine some of the unusual properties of helicenes in depth.

The observation that known helicenes, including penta- to nonahelicenes and several heterohelicenes,[3] crystallize as conglomerates, that is, enantiomorphic crystals in non-centrosymmetric space groups, suggested that new methods for the resolution of conglomerates[4] might prove useful for this class of compound. With an eye toward future applications, it would be useful to prepare a helicene that contains a functional group that allows further derivatization or immobilization.

A short, efficient synthesis of 5-aminohexahelicene has been developed. This compound is racemic rather than a conglomerate in the three-dimensional (3D) crystal, but a conglomerate in two dimensions (2D) at the liquid–solid interface on gold.[3] The absorption of this molecule on Au(111) surfaces under high-vacuum conditions has also been studied.[5] The synthesis and further examination of the behavior of this compound on surfaces are described herein.

The first synthesis of a helicene molecule was an impressive challenge. Newman and Lednicer reported the preparation of hexahelicene[6] in 1955 in 3.7% overall yield. The resolution had been described a year earlier.[7] Photocyclization routes developed by Martin and Baes[8] and Wynberg,[9] for example, offered much easier access to helicenes, including those with heterocyclic rings. Further developments in the synthetic strategy and structural variation with a strong emphasis on metal-catalyzed reactions was achieved by Stará and Starý[10] and by Storch et al.[11] Other interesting approaches have been developed, for example, by Miller and co-workers[12] and Lacour and co-workers.[13] This chemistry with discussion of other recent methods has been covered in four recent reviews.[14–17]

We wished to develop scalable syntheses by using readily available starting materials and to study the properties, both in

[a] Dr. M. W. van der Meijden, Prof. R. M. Kellogg
Syncom BV, Kadijk 3, 9747 AT Groningen (The Netherlands)
E-mail: r.m.kellogg@syncom.nl

[b] Dr. E. Gelens
Nano Fiber Matrices B.V., Zernikepark 6
9747 AN Groningen (The Netherlands)

[c] Dr. N. M. Quirós, Dr. J. D. Fuhr, Dr. J. E. Gayone, Dr. H. Ascolani
Centro Atómico Bariloche
CNEA and CONICET, Av. E. Bustillo km. 9.500 R8402AGP San Carlos de Bariloche (Argentina)

[d] Dr. N. M. Quirós
Permanent address: Instituto Tecnologico de Costa Rica
A-4, Tecnológico de Costa Rica, Cartago (Costa Rica)

[e] Dr. K. Wurst
Institute of General, Inorganic and Theoretical Chemistry
University of Innsbruck, Innrain 80–82
6020 Innsbruck (Austria)

[f] Dr. M. Lingenfelder
Institut de Physique de la Matière Condensée
École Polytechnique Fédérale de Lausanne
1015 Lausanne (Switzerland)
E-mail: magali.lingenfelder@epfl.ch

Supporting information for this article is available on the WWW under http://dx.doi.org/10.1002/chem.201502798.

3D and 2D, of helicenes that are potentially "tunable" by the introduction of substituents that should affect the electronic and optical properties and also allow further functionalization or immobilization. For these purposes, we chose to prepare an aminohelicene. Maleimide- and maleic anhydride-functionalized pentahelicenes containing a single amino group[18] and a 6,11-bis-acetyl-protected diaminohexahelicene[19] have been reported. To the best of our knowledge, no mono-amino-functionalized carbohelicene has been prepared and studied, although an hydrogenated aminohelicene has been synthesized.[20]

Highly linear syntheses are unattractive; furthermore, shorter syntheses that use, for example, the convergence afforded by modern cross-coupling reactions are more attractive. The position of a substituent is determined by the choice of the starting materials. In a search for short, simple approaches adaptable to scale up, the synthesis of pentahelicene reported by de Koning and co-workers[21] by cross coupling two simple building blocks followed by what, at first sight, looks like straightforward condensation chemistry was appealing (Scheme 1).

Pentahelicene **6** is reported as the major product, consistent with dehydrogenation during ring closure. The authors noted that the mechanism of ring closure may be complex and that success is highly dependent on the conditions. Although cross coupling to provide **5** worked well (52% yield), subsequent ring closure to **6** failed in our hands, either with a base or with a base and irradiation as described by the authors. After several unsuccessful attempts, this approach was abandoned.[22]

Simultaneously, Fürstner and co-workers[23] followed a similar cross-coupling strategy to **6**, but accomplished the final ring closure by clever use of a metal-catalyzed reaction. In our hands, this procedure, carried out without the determination of yields and on a small scale, worked well and provided **6** (Scheme 2).

The half-life of the racemization of pentahelicene at 57 °C is 63 minutes.[24] A higher degree of enantiomeric stability was desired, and the decision was made to prepare a functionalized hexa- rather than a pentahelicene. Hexahelicene has a half-life of racemization of 48 minutes at 205 °C.[25] The obvious starting materials are boronic acid or ester **10** and bromoenol **11** (Scheme 3). The placement of the amino substituent at position 5 of the hexahelicene skeleton lies in the choice of readily available **10** as a starting material.

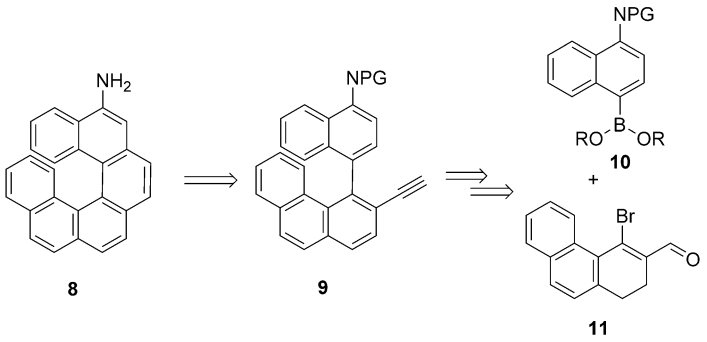

Scheme 3. Retrosynthesis of aminohexahelicene (**8**). PG = protecting group.

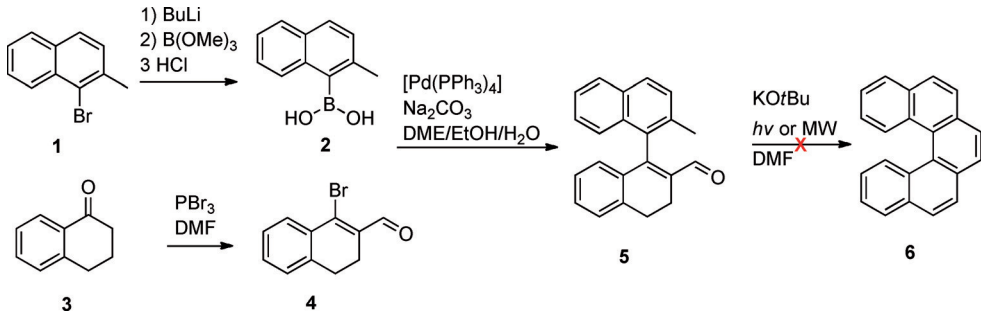

Scheme 1. Synthesis of pentahelicene according to de Koning et al.[21] DME = dimethyl ether, MW = microwave.

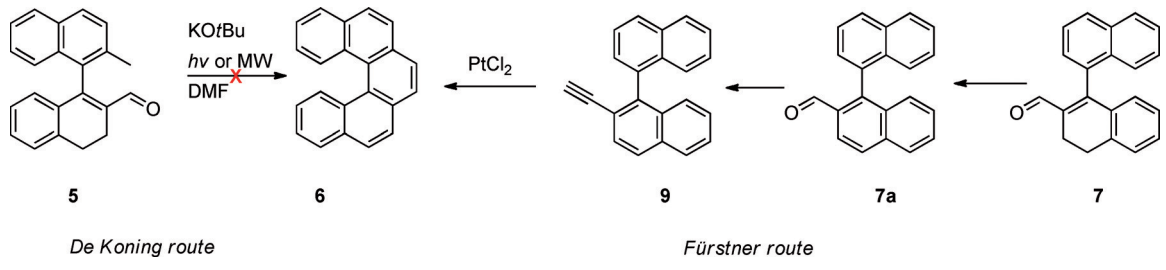

Scheme 2. Comparison of the routes of de Koning[21] and Fürstner.[23]

Results and Discussion

Compounds **10a** and **10b** were obtained from commercially available 4-bromo-1-naphthylamine (**12**). The *tert*-butoxycarbonyl (Boc) group was chosen for protection because there are no steps that involve acid until deprotection under acidic conditions.

Initially, the protection of **12** with $(Boc)_2O$ was performed without a base and gave **13** in only 64% yield (Scheme 4). However, when the reaction was performed with two equivalents of base and a large excess of Boc_2O was added in two portions,[26] an 88% yield could be obtained. Bromide **13** was then converted into either boronic acid **10a** or boronic ester **10b**. The best results were obtained with MeLi followed by a bromo–lithium exchange by using *n*BuLi. Quenching with $B(OEt)_3$ and subsequent hydrolysis gave the desired boronic acid **10a**,[27] which could be used as the crude product in the next step. Standard conditions (i.e., bispinacolato diboron, $[PdCl_2(dppf)_2]$, CH_2Cl_2/KOAc) were used to prepare boronic ester **10b** in 62% yield.

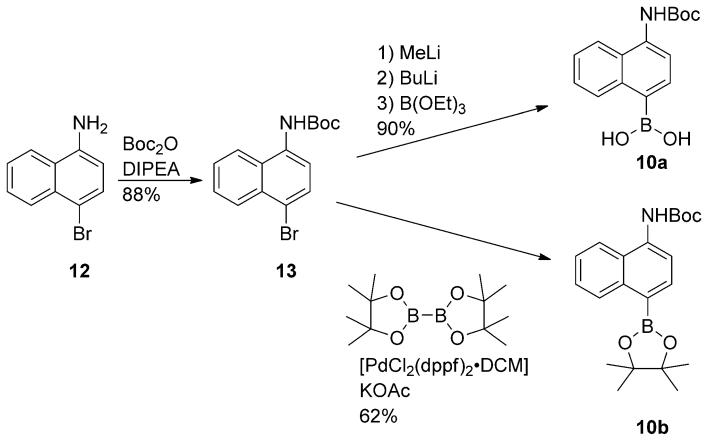

Scheme 4. Synthesis of the upper part of the helicene skeleton. DCM = dichloromethane, DIPEA = *N*,*N*-diisopropylethylamine, dppf = 1,1′-bis(diphenylphosphino)ferrocene.

For the synthesis of bromoaldehyde **11**, ketone **14** was required (Scheme 5). Although phenanthrenone (**14**) is commercially available, it is expensive. Because appreciable amounts were needed, it was decided, after ensuring that the conversion of **14** into **11** proceeded well by using a small amount of purchased material, to prepare **14** from naphthalene (**15**) and succinic anhydride (**16**; Scheme 6). Keto ester **17** was obtained in 31–42% yield. This reaction has been reported several times.[28–30] The procedure of Wiznycia and Desper[30] was chosen because of the facile workup.

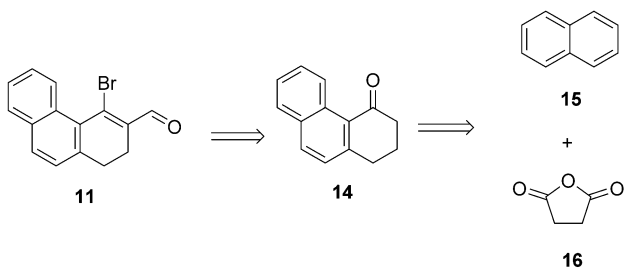

Scheme 5. Retrosynthesis of bromoenol **11**.

The reduction of keto-ester **17** under Wolff–Kishner conditions was irreproducible. An excellent alternative was reduction under mild conditions (slight positive H_2 pressure at ambient temperature) with $Pd(OH)_2$ in acetic acid.[31] The desired **18** was obtained in 73–75% yield. Direct conversion of naphthalene (**15**) into acid **18** by the Friedel–Crafts reaction with butyrolactone,[32,33] either neat, in *n*-decane, or in nitrobenzene, did not give satisfactory results. The ring closure of **18** by using neat methanesulfonic acid at 90 °C was fast and effective and gave **14** in 83–95% yield.[34] The final step is a combined enolization and Vilsmeier–Haack reaction to give **11** by following the procedure by de Koning et al. for the tetralone derivative.[21] This compound is not very stable and should be used immediately or stored in the freezer. By using this route, considerable amounts of **11** (i.e., we prepared 16.5 g) can be synthesized in a short time and from cheap starting materials, without the use of expensive reagents or harsh conditions.

The coupling of boron compound **10** and bromo aldehyde **11** was achieved (Scheme 7) by using a Suzuki coupling.

The conditions reported by Fürstner and co-workers[23] (i.e., $Pd(OAc)_2$, tetrabutylammonium bromide, K_2CO_3, water) were first investigated, but this gave 3% yield at best after multiple purifications. Large amounts of starting material were recovered. Steric hindrance in combination with the low solubility in water was a possible cause. Recourse was found in $Pd(OAc)_2$ with *S*-phos, a catalyst that was designed for sterically demanding compounds.[35] No reaction occurred with boronic ester **10b**, whereas yields of **19** of 75–95% were obtained with boronic acid **10a**.

The synthesis of the desired 5-amino[6]hexahelicene **8** is shown in Scheme 8. For the aromatization of the dihydro ring of **19**, the use of 2,3-dichloro-5,6-dicyano-1,4-benzoquinone (DDQ)[23] was first investigated, but this reaction was slow. *N*-Bromosuccinimide (NBS)/Na_2CO_3,[36] NBS/1,8-diazabicyclo[5.4.0]undec-7-ene (DBU), and diethyl azodicarboxylate (DEAD) were examined as alternatives, but all failed to give good results. After some experimentation, it was found that the DDQ dehydrogenation in benzene proceeded usually in approximately 75% yield, if given sufficient time (i.e., 3 days). Change of the solvent from benzene to less harmful toluene led to no reaction at all.

Aldehyde **20** was converted into alkyne **9** by means of the Ohira–Bestmann modification of the Seyfert–Gilbert homologation.[37] This method led to the desired alkyne **9** in good yields (69–91%). In theory, cyclization of alkyne **9** to **21** is possible with a variety of metal species.[38] First, $PtCl_2$ and $AuCl_3$ were tested, and the former gave the best results (60–96% yield). The mechanism according to Nevado and Echavarren[39] and Soriana and Marco-Contelles[40] involves a Friedel-Crafts reac-

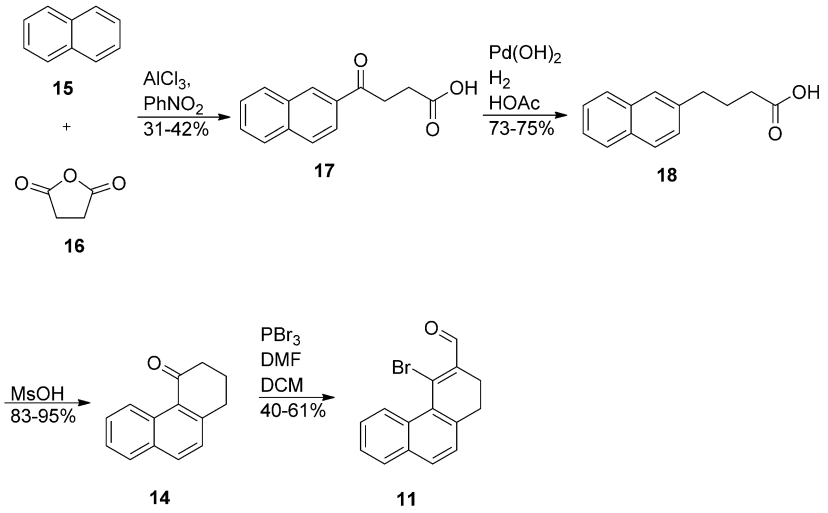

Scheme 6. Synthesis of the lower part of the helicene skeleton. MsOH = methanesulfonic acid.

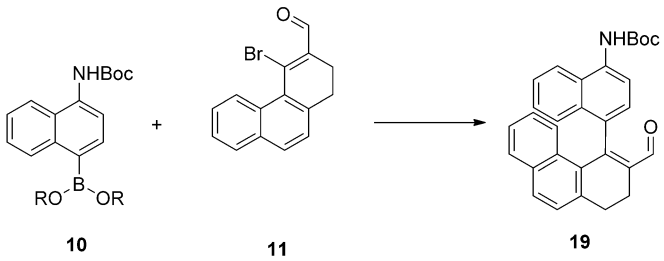

Scheme 7. Suzuki coupling of the upper- and lower parts of the helicene skeleton (see text for the conditions).

tion with 6-*endo*-dig cyclization (see the Supporting Information). The 5-*exo*-product is also a possible product, although this material was never observed (see the Supporting Information). Attempts were made to achieve enantioselective ring closure by using various popular enantiopure ligands (see the Supporting Information); unfortunately, no enantioselectivity was observed.

To obtain the desired helicene **8**, the Boc-protecting group was removed with HCl and the salt liberated with $NaHCO_3$. The overall route is relatively short, simple, and proceeds under mild conditions in about 50% overall yield by starting from boronic acid **10a**. This novel approach allows the preparation of multigram quantities of the desired functionalized helicene, which should be stored as the hydrochloric acid salt **22** or Boc-protected helicene **21** to avoid byproduct formation, likely owing to oxidation of the amine.

Resolution and physical properties of aminohelicene (8)

Dibenzoyl tartaric acid, ditoluyl tartaric acid, dianisoyl tartaric acid, tartaric acid, camphorsulfonic acid, phencyphos,[41] and P-Mix (i.e., a mixture of phencyphos, chlocyphos, and anisyphos)

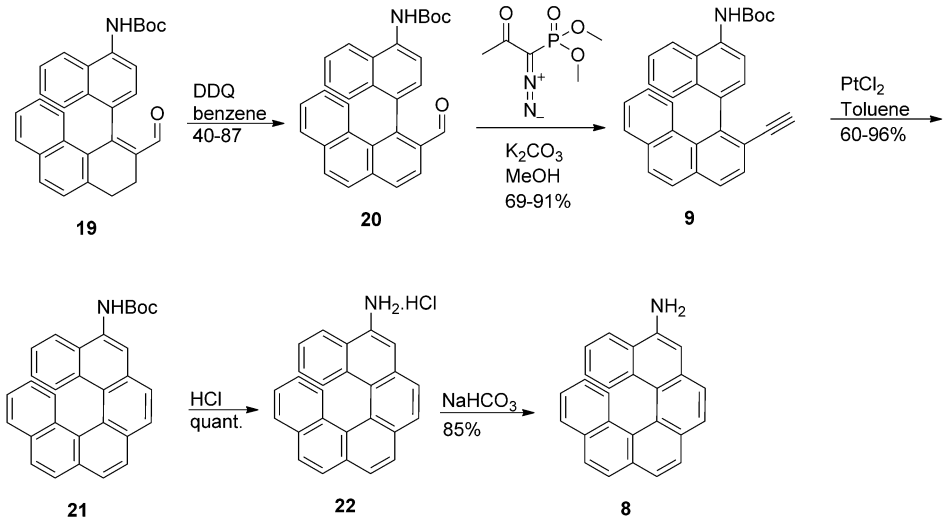

Scheme 8. Synthesis of final product **8** from **19**.

were all tested as resolving agents for **8**.[42] As solvents, EtOH/water, DMF/water, 2-butanone, toluene, CH_3CN, EtOAc, and $MeNO_2$ were used. In all cases, except for in DMF/water, the solubilities were poor and crystallization was very fast. In the experiments with DMF/water as a solvent, no crystallization occurred, even after prolonged standing. Neutralization of the salts failed to provide **8** with any significant enantiomeric excess. The failure to obtain any resolution may be due low solubility, which leads to crystallization before the thermodynamic equilibrium can be reached. Separation into enantiomers was possible on a small scale with the aid of preparative HPLC (see the Experimental Section).

The $t_{1/2}$ value for the racemization of hexahelicene, as determined by CD spectroscopic analysis, is 48 minutes at 205 °C.[25,43] In similar experiments with **8**, a solvent that has a boiling point above 200 °C and limited or no UV absorption was required; therefore, 1,3-dimethyl-3,4,5,6-tetrahydro-2(1*H*)-pyrimidinone (DMPU; b.p. 246 °C) was chosen. The change in the CD spectrum as function of temperature followed (see the Supporting Information). The $t_{1/2}$ value for racemization is approximately 1 hour at 210 °C, which means that racemization would take 2–3 hours at 200 °C and 6–7 hours at 180 °C.

The CD spectra of the enantiomers of **8** are shown in Figure 1. Based on the close similarity to the CD spectrum of hexahelicene itself,[44] the right-handed *P* helicity was assigned to the (+) enantiomer. The optical rotation was determined with material that was not entirely pure (see the Supporting Information); that is, the observed rotation was $[\alpha]_D = -8846°$ for the (−) enantiomer, which had a chemical purity of 93% and an *ee* value of 99%, whereas the observed rotation was $[\alpha]_D = +7429°$ for the less pure (+) enantiomer (chemical purity = 83%, *ee* = 97%). A corrected rotation for **8** by using the material of peak 1 would be 9511°, if one assumes that the impurities (likely to be the oxidation products of **8**) have no appreciable CD spectrum.

Second harmonic generation (SHG) experiments carried out on **8** led to no response, thus strongly suggesting that **8** is not a conglomerate, but rather a centrosymmetric racemic compound (or amorphous). Crystal-structure determination revealed the compound to have a racemic crystal structure (Figure 2).[44] The space group was found to be *Pbcn*, which is consistent with a centrosymmetric structure (i.e., racemic compound and not a conglomerate).

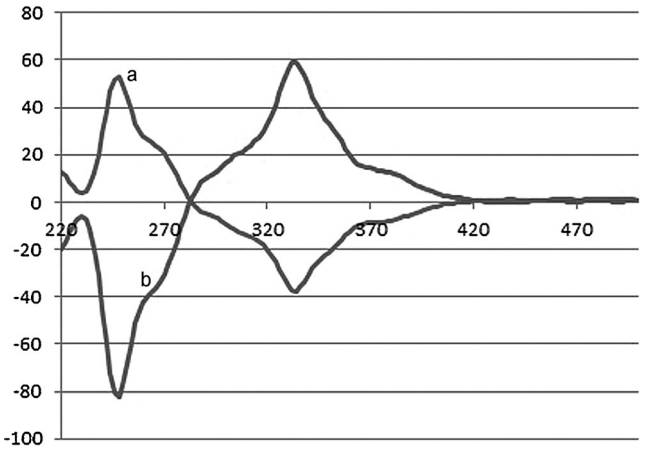

Figure 1. CD spectrum of both peaks of aminohexahelicene (**8**; a) (−)-aminohexahelicene: $c = 0.013$ mmol L^{-1} in MeOH; b) (+)-aminohexahelicene: $c = 0.006$ mmol L^{-1} in MeOH).

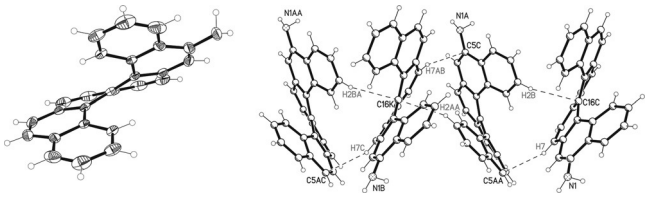

Figure 2. X-ray structure of aminohelicene (**8**). Left: ORTEP of the molecular structure with ellipsoids at the 50% level. Right: Alignment of alternate enantiomers along the *a* axis. Intermolecular hydrogen–π_{carbon} interactions are drawn with dashed lines.

STM analysis

In the 3D crystal, aminohelicene **8** (AH) does not form a conglomerate. Confinement in 2D leads to a decrease of the number of allowed space groups from 230 to 17, and there are only five possible 2D chiral space groups.[45] Therefore, there is a large chance of the loss of symmetry elements because of adsorption on a surface, there is a much larger probability of spontaneous separation of the enantiomers into separate domains (i.e., conglomerate formation) than for a 3D system.[45] STM studies at the liquid–solid interface[3] have demonstrated that aminohelicene **8** on Au(111) can coexist as enantiomerically pure conglomerates and enantiomorphous racemates. Herein, we present the first study of the assembly and chiral expression of racemic AH under ultrahigh vacuum (UHV) conditions.

To investigate the crystallization properties of AH when it is confined to a 2D surface, we deposited both the (*M*)-AH enantiomer and racemate on Au(111) under UHV conditions. All molecular depositions were done at room temperature (RT) and the images were acquired at 100 K.

We observed that the enantiomer develops two rotational domains formed by rows of dimers oriented along the $<1-11>$ Au crystallographic directions (Figure 3a)). These structures were described recently by DFT calculations as being formed by flat-lying molecules in which the $-NH_2$ groups govern the interaction with the surface (i.e., "N down"), whereas the C_6 rings pack closely to maximize van der Waals interactions between neighboring molecules. The double-row structure (inset in Figure 3a) shows the higher packing density and is favored at high coverage, but always coexists with disordered inter-island regions in which dimers, trimers, and tetramers of molecules are embedded.[4]

Herein, we show that the assembly of the racemate gives rise to a new structure, which is remarkably different to the enantiomer islands. Figure 3b shows that two enantiomorphous domains emerge rotated by $\pm 6°$ (gray arrows) with respect to the $<1-11>$ crystallographic directions (black arrows). Interestingly, the molecular structure produced by the racemate comprises two nonequivalent rows that alternate

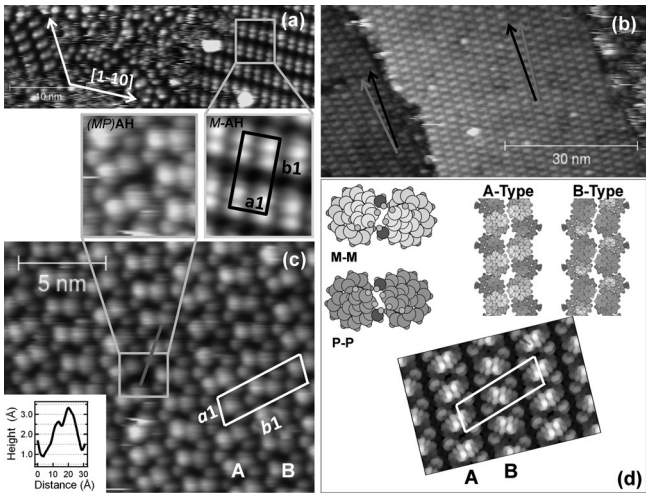

Figure 3. a) STM image of (*M*)-AH on Au(111) (+2 V, 20 pA). b, c) STM images of racemic AH on Au(111). b) Two enantiomorphous domains separated by a monoatomic step of the surface. (−2 V, 5 pA). c) High-resolution image (−2 V, 5 pA) of the molecular structure developed by the racemate. The white parallelogram indicates the unit cell. The square highlights the presence of a defect (zoomed in the inset). The gray line indicates the line profile shown in the inset. d) DFT-based molecular model of the racemic structure in (c) that highlights the presence of *M*–*M* and *P*–*P* dimers in the A- and B-type molecular-row model. Different colors indicate different chirality: Light gray for (*M*)-AH and dark gray for (*P*)-AH. Constant-current STM image simulation (−2 V) of the fully relaxed structure (Figure S5 in the Supporting Information).

systematically in a zigzag fashion labeled "A" and "B" in Figure 3c[46] (the unit cell is indicated by a white parallelogram ($a1 = (1.4 \pm 0.1)$, $b1 = (4.5 \pm 0.1)$ nm; $a1 \wedge b1 = 74 \pm 2^\circ$). The internal structure of these rows appears to be more complex than for the (*M*)-AH enantiomer. Clearly, the STM contrast evidences two types of protrusions of distinct volume, that is, large and bright regions and small and dim regions (Figure 3c). This type of contrast is reproduced systematically on different (*M*/*P*)-AH samples under various tip conditions. Initially, one might be tempted to correlate the two features with the bright and dim lobes observed by Ernst et al. in the high-resolution STM images of single heptahelicene molecules.[47] However, the small protrusions were never observed in enantiopure samples of AH. This finding, along with the observation of small and/or large protrusion vacancies in different islands (Figure 3c) shows a zoomed region in which a defect is observed; see also Figure 1 in the Supporting Information for further examples), allows us to conclude that the bright and dim features are independent molecules in this system that might correspond to two molecules absorbed in different configurations. After analyzing numerous images taken under different tip conditions, we assign the observed difference of 0.7 Å in the apparent heights (see the line profile in Figure 3) to a difference in the real height of the adsorbed molecules. To propose a model that will be consistent with these observations, we carried out a series of DFT calculations and STM simulations of the appearance of the molecules under the applied experimental conditions (see Figure S2 in the Supporting Information). By taking into account the minimum energy structures for different *M*/*P* configurations for both N-down (see Section 2.2.1) and N-up adsorption geometries (see Section 2.2.2), we found that the rows can be described as a sequence of dimers formed by large protrusions (N-up) and connected by small protrusions (N-down).

The calculated model is based on the following assumptions: 1) the different apparent heights are due to molecules with two different configurations (see Figure S3 in the Supporting Information), 2) the lower molecules interact with the substrate in th N-down configuration (see Section 2.3), 3) the observed higher dimers consist of N-up dimers formed with molecules of the same chirality (i.e., *M*–*M* or *P*–*P* molecules; Figure 3d). *M*–*P* dimers have a similar interaction energy, but they cannot reproduce the symmetric aspect of the observed dimers (see Section 2.2.2). The structural model consists of rows formed by the mentioned N-up dimers, linked by N-down molecules of the opposite chirality (Figure 3d; the (*M*)-AH and (*P*)-AH molecules are colored yellow and green, respectively). The dimers are *M*–*M* in the A-type row, whereas the dimers are *P*–*P* in the B-type row. In both cases, the molecules that form the dimers (N-up orientation) are slightly higher from the surface (see the lateral view in given in Figure S5 in the Supporting Information). The higher molecules interact with those located lower through an intermolecular interaction similar to that observed in lamellar twinning,[48] that is, part of the helix of one molecule interlocks with the helix of the nearest neighbor. The unit cell contains eight AH molecules in two types of configuration, thus giving a lateral average area per molecule of 77 Å^2, which is a very high packing density that is consistent with the high coverage needed to observe the self-assembled structure.

We relaxed the complete structure, thus fixing the unit cell to the cell observed in the experiments to investigate the stability of the A–B row model (see Figure S5 (upper panel) in the Supporting Information). Furthermore, to simulate the absorption on the surface, we constrained the *z* position of the two lower C rings only on the N-down molecules. After relaxing the molecular configuration, we obtained an interaction-energy value per unit cell of 4.32 eV, that is, 0.54 eV per molecule. Remarkably, this value for the interaction energy per molecule is the highest found within all the molecular configurations analyzed herein, including dimers, zigzag chains, and so forth (see Section 2.2). Although the absolute energy values are expected to be modified by the interaction with the Au surface, the interaction energy calculated for the A–B row model is the most favorable from the point of view of the molecular-interaction energy. Moreover, we simulated a constant-current STM image by using this relaxed-structure model (Figure 3d). This simulated STM image agrees with the main features of the experimentally obtained image: 1) there are two spots in each row that are brighter and bigger, which, in the model, correspond to the N-up molecules in the dimer; 2) there are smaller and darker protrusions at each side of the main protrusions that correspond to the N-down molecules that link the dimers.

It was noticed that the assembly of double rows under UHV (see Figure 3a and reference [4]) is remarkably different to the

triangular (p3) structures formed at the Au(111)/1,2,4-trichlorobenzene (TBC) interface.[3] At the liquid–solid interface, the assembly depends drastically on the solvent, most likely due to its role in the determination of the protonation state of the $-NH_2$ group. In fact, no order emerges in solvents in which the NH_2 group is protonated, whereas the assembly is very similar to that observed for the nonfunctionalized heptahelicene on Au(111) in neutral solvents.[49] For the racemate, incomplete spontaneous resolution was proposed to be a consequence of kinetic trapping of metastable racemic polymorphs due to slow surface diffusion. The high packing density of the racemate and the absence of enantiopure phases indicate that the driving force for the assembly under UHV conditions is probably related to the thermodynamic stability of the phase, similar to the 3D crystal in which the racemate is more stable, and therefore no resolution occurs.

Conclusion

The cross-coupling synthetic strategy followed to obtain helicene **8** has made use of readily accessible and not excessively expensive building blocks. Monoamino hexahelicenes bearing the amino group at the 1, 2, 3, or 4 position have become potentially available due to a corresponding change in the structure of building block **10**. We did not attempt this approach owing to project restrictions. Hexahelicene **8** and other amino derivatives, if prepared on a moderate scale, could be subject to conversion into other derivatives by replacement of the amino group through diazonium chemistry. This approach opens a route to a range of helicenes that can be investigated for applications. One could also consider the attachment of the amino group of the helicene to, for example, a silicon surface by reaction with an isocyanide-functionalized surface to investigate optical and electronic properties. In conclusion, we have been able to prepare a new functionalized helicene that can be used for further investigation of its properties and that could be further functionalized or immobilized. The compound proved to form racemic phases both in the solid state and when immobilized on a Au(111) surface under UHV conditions.

Experimental Section

The NMR spectra were measured at ambient temperature on a Varian VNMRS 300 MHz or a Varian MercuryPlus 300 MHz spectrometer. $CDCl_3$ and [D_6]DMSO were used as solvents and as indicated. The HPLC-MS spectra were measured on an Agilent 1100 series with a UV detector and HP1100 MSD mass detector, an Agilent 1200 series with a UV detector and Agilent 6130 mass detector, or an Agilent 1200 series with a UV detector and 6220 TOF mass detector. Enantiomeric separation was accomplished by means of HPLC on a Chiralcel OD-H column and subsequently tested by HPLC analysis.

***tert*-Butyl 4-bromonaphthalen-1-yl carbamate (13)**: A mixture of bromide **12** (100 g, 450 mmol), DIPEA (149 mL, 900 mmol, 2 equiv), and Boc_2O (147.4 g, 675 mmol, 1.5 equiv) was heated to reflux in 1,2-dichloroethene (DCE; 2 L) for 4 h. Boc_2O (393.0 g, 1.8 mol, 4 equiv) was added to the reaction mixture, which was heated overnight to reflux. TLC analysis in dichloromethane (using UV detector) revealed almost complete conversion, the mixture was washed with 2 M HCl (350 mL), saturated $NaHCO_3$ (350 mL), and water (250 mL). The organic layer was dried over Na_2SO_4 and concentrated. The resulting material was recrystallized from heptane (1.3 L), cooled with ice, and collected by filtration. The solids were washed with heptane, dissolved in dichloromethane and filtered over SiO_2 (0.5 L, dichloromethane) to give carbamate **13** as a white solid (128.2 g, 88% yield). ^{1}H NMR ($CDCl_3$): $\delta = =8.27$ (d, 1H), 7.88 (d, 1H), 7.78 (m, 2H), 7.60 (m, 2H), 6.82 (br s, 1H), 1.55 ppm (s, 9H); ^{13}C NMR ($CDCl_3$) $\delta = 153.4$, 133.2, 133.2, 132.5, 130.0, 128.3, 127.9, 127.5, 127.0, 121.1, 119.3, 99.5, 81.3, 28.6 ppm; MS (API/ES): *m/z*: 344.03 [*M*+Na]; found: 343.9.

4-(*tert*-Butoxycarbonylamino)naphthalen-1-yl boronic acid (10a): Bromide **13** (14.6 g, 45.3 mmol) in THF (95 mL) was placed in a flame-dried flask with mechanical stirring and the mixture was cooled to 0 °C. MeLi (1.6 M in Et_2O, 28.3 mL, 45.3 mmol, 1 equiv) was added at such a rate that $T<7$ °C, the temperature was kept at 0 °C for 15 min, and lowered to −78 °C. BuLi (2.5 M in hexanes, 18.1 mL, 45.3 mmol, 1 equiv) was added at such a rate that $T<$ 70 °C, the mixture was stirred for 1 h at −78 °C, and $B(OEt)_3$ (19.3 mL, 113 mmol, 2.5 equiv) was added subsequently at such a rate that $T<-65$ °C and gelation of the mixture occurred. The mixture was stirred for 45 min at −78 °C and then for 1.5 h at 0 °C. HCl (1 M, 125 mL) was added carefully with ice cooling, and the mixture was stirred for 15 min after removal of the cooling bath. The mixture was saturated with NaCl and the layers were separated. The organic layer was extracted with 1 M NaOH (4×125 mL), and the combined basic, aqueous layers were acidified under ice cooling with 5% HCl. The mixture was extracted with Et_2O (3× 125 mL), dried over Na_2SO_4, and concentrated at 25 °C to give boronic acid **10a** as a white solid containing a few minor impurities (11.7 g, 90% yield). ^{1}H NMR ([D_6]DMSO): $\delta = 9.24$ (s, 1H), 8.41 (m, 1H), 8.27 (s, 2H), 8.05 (m, 1H), 7.69 (d, 1H), 7.52 (d, 2H), 7.50–7.43 (m, 2H), 1.48 ppm (s, 9H); ^{13}C NMR ($CDCl_3$): $\delta = 154.7$, 138.2, 137.2, 135.9, 132.8, 129.7, 128.2, 126.2, 125.6, 123.5, 120.5, 79.6, 28.9 ppm; MS (API/ES): *m/z*: 310.12 [*M*+Na]; found: 310.0.

4-(Naphthalen-2-yl)-4-oxobutanoic acid (17): A mixture of naphthalene **15** (210 g, 1.64 mol, 1.5 equiv) and succinic anhydride **16** (109.3 g, 1.09 mol) was added in one portion to a solution of $AlCl_3$ in $PhNO_2$ (900 mL) under N_2 with mechanical stirring. The resulting mixture was stirred overnight at RT and poured into ice/water (2.5 L). A mixture of water (100 mL) and 37% HCl (100 mL) was added to the mixture. The resulting precipitate was collected by filtration and washed with water (1.2 L) and heptane (450 mL). The solid was stirred for 0.5 h at 65 °C in toluene (900 mL), was cooled to approximately 35 °C, collected by filtration, and washed with toluene to give ketoacid **17** as a tan solid (104.6 g, 42% yield). ^{1}H NMR ($CDCl_3$): $\delta = 8.51$ (1H, s), 8.06 (1H, d), 8.00 (1H, d), 7.89 (2H, t), 7.56–7.64 (2H, m), 3.5 (2H, t), 2.9 ppm (2H, t); ^{13}C NMR ($CDCl_3$) $\delta = 198.0$, 177.6, 136.0, 134.0, 132.7, 130.1, 129.8, 128.8 (d), 128.0, 127.1, 123.9, 33.5, 28.2 ppm; MS (API/ES): *m/z*: 227.08 [*M*−1]; found: 227.1.

4-(Naphthalen-2-yl)butanoic acid (18): Ketoacid **17** (104.6 g, 458 mmol) and $Pd(OH)_2/C$ (10 g) were stirred in HOAc (1 L). The mixture was flushed three times with H_2 and then stirred under a balloon of H_2 at RT while monitoring the conversion by means of NMR spectroscopic analysis. Complete conversion was observed after 2 days, and the mixture was filtered over celite and washed with HOAc (200 mL). The mother liquor was poured into cold water (4 L) and the resulting precipitate was collected by filtration and washed with toluene to give acid **18** as a white solid (71.6 g, 73% yield). ^{1}H NMR ($CDCl_3$): $\delta = 7.74$ (3H, t), 7.62, (1H, s), 7.42–7.46 (2H, m), 7.33 (1H, d), 2.85 (2H, t), 2.42 (2H, t), 2.06 ppm (2H, q);

^{13}C NMR ($CDCl_3$): δ = 128.3, 127.8, 127.7, 127.4, 126.9, 126.2, 125.5, 35.4, 33.4, 26.3 ppm; ^{13}C NMR ($CDCl_3$): δ = 180.6, 139.0, 133.9, 132.4, 128.3, 127.9, 127.8, 127.5, 126.9, 129.3, 125.6, 35.4, 33.7, 26.3 ppm; MS (API/ES): *m/z*: 213.10 [*M*−1]; found: 213.0.

2,3-Dihydrophenanthren-4(1*H*)-one (14): MsOH (375 mL) was stirred at 90 °C and acid **18** (71.6 g, 107 mmol) was added in one portion. The mixture was stirred for 1 h at 90–95 °C and was subsequently cooled to RT. The mixture was poured slowly in ice/water (4.5 L) and extracted with Et_2O (3×750 mL). The combined organic layers were washed with $NaHCO_3$ (750 mL) and water (750 mL), dried over Na_2SO_4, and concentrated to give ketone **14** as a brown oil, which crystallized upon standing (62.2 g, 95% yield). ^{1}H NMR ($CDCl_3$): δ = 9.41 (1H, d), 7.92 (1H, d), 7.81 (1H, d), 7.63 (1H, t), 7.49 (1H, t), 7.32 (1H, d), 3.13 (2H, t), 2.79 (2H, t), 2.15–2.24 ppm (2H, m); ^{13}C NMR ($CDCl_3$): δ = 200.7, 147.0, 134.4, 133.0, 131.6, 129.0, 128.5, 127.5, 127.2, 126.9, 126.0, 41.3, 31.8, 23.2 ppm; MS (API/ES): *m/z*: 197.09 [*M*+1]; found: 197.1.

4-Bromo-1,2-dihydrophenanthrene-3-carbaldehyde (11): PBr_3 (28.7 mL, 306 mmol, 2.4 equiv) was added dropwise to dry DMF (28.6 mL, 369 mmol, 2.9 equiv) in dry dichloromethane (550 mL) at 0 °C. Ketone **14** (25 g, 127 mmol) in dry dichloromethane (475 mL) was added in one portion after 1 h at 0 °C. The mixture was heated to reflux overnight. The reaction mixture was cooled with ice/MeOH, saturated $NaHCO_3$ was added to make the mixture basic, and the layers were separated. The aqueous layer was extracted with dichloromethane (750 mL) and the combined organic layers were washed with water (400 mL), dried over Na_2SO_4, and concentrated to give the crude aldehyde **11** (20 g). The obtained material was purified by column chromatography over SiO_2 (1 kg; eluent = EtOAc/heptane 1:9) to give aldehyde **11** as a yellow oil (15.6 g, 43% yield). ^{1}H NMR ($CDCl_3$): δ = 10.33 (1H, s), 8.71 (1H, s), 7.85 (2H, s), 7.47–7.60 (2H, m), 7.34 (1H, d), 2.85 (2H, t), 2.60 ppm (2H, t); ^{13}C NMR ($CDCl_3$) δ = 192.9, 141.1, 138.1, 135.8, 134.0, 132.0, 130.5, 130.3, 129.0, 126.6, 126.0, 125.9, 125.6, 29.9, 22.9 ppm; MS (API/ES): *m/z*: 287.00 [*M*+1]; found: 287.1.

***tert*-Butyl 4-(3-formyl-1,2-dihydrophenanthren-4-yl)naphthalen-1-yl carbamate (19)**: Bromide **11** (15.6 g, 54 mmol) in toluene (300 mL) was placed in a flame-dried flask, and N_2 was bubbled through the mixtue for 10 min. A few drops of water were added to the reaction mixture, followed by K_3PO_4(23.1 g, 109 mmol, 2 equiv), boronic acid **10a** (23.4 g, 81 mmol, 1.5 equiv), $Pd(OAc)_2$ (122 mg, 0.5 mmol, 1 mol%), and *S*-Phos (558 mg, 1.4 mmol, 2.5 mol%). The resulting mixture was heated to reflux overnight. TLC analysis (eluent: EtOAc/heptane 2:8, detection: UV/CeMo dip) revealed complete conversion. Water (750 mL) was added to the mixture, which was extracted with EtOAc (2×750 mL). The combined organic layers were washed with water (500 mL), dried over Na_2SO_4, and concentrated to give the crude coupled product (35 g). The obtained material was purified over SiO_2 (1 kg; eluent: EtOAc/heptane 1:9) to give aldehyde **19** as a yellow product, which was not pure according to TLC analysis, but contained only a few minor impurities as determined by NMR spectroscopic analysis (22.0 g, 91% yield). ^{1}H NMR ($CDCl_3$): δ = 9.52 (s, 1H), 8.07 (d, 1H), 7.86 (dd, 2H), 7.69 (d, 1H), 7.59 (d, 1H), 7.49–7.41 (m, 3H), 7.29 (d, 1H), 7.16 (t, 2H), 7.01 (br s, 1H), 6.81 (t, 1H), 3.07 (t, 2H, 2.89–2.84 (m, 1H), 2.74–2.63 (m, 1H), 1.59 ppm (s, 9H); ^{13}C NMR ($CDCl_3$): δ = 193.6, 153.4, 152.2, 140.2, 137.9, 134.3, 133.9, 133.4, 132.1, 131.8, 131.6, 131.5, 129.5, 129.0, 128.3, 127.7, 127.1, 126.7, 126.3, 126.1, 125.1, 125.0120.8, 116.9, 81.3, 30.6, 28.6, 20.6 ppm; MS (API/ES): *m/z*: 448.20 [*M*−1]; found: 448.2.

***tert*-Butyl 4-(3-formylphenanthren-4-yl)naphthalen-1-yl carbamate (20)**: DDQ (13.9 g, 61 mmol, 1.25 equiv) was added to alkene **19** (22.0 g, 49 mmol) in benzene (1.5 L) and heated to reflux over the weekend. NMR spectroscopic analysis revealed complete conversion. The mixture was cooled to RT and filtered over celite. The residual solids were washed with toluene, and the mother liquor with 1 M NaOH (3×1 L). The combined aqueous layers were extracted with toluene (1 L), dried over Na_2SO_4, and concentrated to give biaryl compound **20** as a brown solid, which was used as such in the next reaction (16.7 g, 76% yield). ^{1}H NMR ($CDCl_3$): δ = 9.48 (s, 1H), 8.28 (d, 1H), 8.19 (d, 1H), 8.09 (t, 2H), 7.80–7.91 (m, 3H), 7.48–7.57 (m, 2H), 7.38 (m, 3H), 7.29 (t, 1H), 7.18 (br s, 1H), 7.93 (t, 1H), 1.63 ppm (s, 9H); ^{13}C NMR ($CDCl_3$) δ = 193.1, 153.5, 143.1, 137.4, 134.7, 134.2, 133.9, 133.8, 132.8, 131.2, 131.1, 130.0, 129.8, 129.2, 128.8, 127.5, 127.4, 127.3, 127.0, 126.7, 126.6, 124.3, 121.0, 117.7, 81.3, 28.7 ppm; MS (API/ES): *m/z*: 470.17 [*M*+Na]; found: 470.1.

***tert*-Butyl 4-(3-ethynylphenanthren-4-yl)naphthalen-1-yl carbamate (9)**: K_2CO_3 (10.8 g, 78.4 mmol, 2.1 equiv), followed by dimethyl 1-diazo-2-oxopropylphosphonate (9.5 g, 49.6 mmol, 1.33 equiv), was added to aldehyde **20** (16.7 g, 37.3 mmol) in MeOH (735 mL). The resulting mixture was stirred overnight at RT, after which NMR spectroscopic analysis revealed complete conversion. Heptane (900 mL), saturated $NaHCO_3$ (900 mL), EtOAc (1.8 L), and water (1.8 L) were added to the reaction mixture. The layers were separated and the aqueous layer was extracted with EtOAc (900 mL). The combined organic layers were dried over Na_2SO_4 and concentrated to give the crude alkyne (17.6 g). This material was purified over SiO_2 (1 L; eluent: EtOAc/heptane 2:8) to give alkyne **9** as a yellow solid (15 g, 91% yield). ^{1}H NMR ($CDCl_3$): δ = 8.12 (br d, 1H), 7.97 (q, 2H), 7.80 (q, 4H), 7.30–7.53 (m, 5H), 7.26 (m, 1H), 7.05 (br s, 1H), 6.88 (t, 1H), 2.73 (s, 1H), 1.62 ppm (d, 9H); ^{13}C NMR ($CDCl_3$): δ = 153.7, 141.5, 137.1, 133.8, 133.7, 133.3, 132.8, 130.4, 130.1, 129.1, 128.8, 128.5, 128.3, 127.6, 127.5, 126.9, 126.6, 126.5, 126.4, 126.2, 123.8, 120.8, 118.4, 114.4, 83.6, 82.0, 81.0, 28.7 ppm; MS (API/ES): *m/z*: 444.19 [*M*+1]; found: 444.3.

5-Boc-aminohexahelicene (21): Alkyne **9** (5.0 g, 11.3 mmol) and $PtCl_2$ (290 mg, 1.1 mmol, 10 mol%) were stirred overnight in toluene (415 mL) at 80 °C, after which NMR spectroscopic analysis revealed complete conversion. The mixture was concentrated and triturated from EtOAc/heptane (2:8) to give helicene **21** as a yellow/orange solid (4.8 g, 96% yield). ^{1}H NMR ($CDCl_3$): δ = 8.49 (br s, 1H), 7.88–8.00 (m, 5H), 7.82 (t, 2H), 7.69 (d, 1H), 7.59 (d, 1H), 7.17–7.29 (m, 3H), 7.11 (br s, 1H), 6.63–6.72 (m, 2H), 1.65 ppm (m, 9H); ^{13}C NMR ($CDCl_3$): δ = 153.7, 132.9, 132.0, 132.0 (2nd), 131.8, 131.6, 130.8, 130.1, 128.8, 128.0, 127.9, 127.7, 127.6, 127.5, 127.2, 127.0, 126.5, 125.9, 125.6, 125.3, 124.9, 124.8, 124.2, 122.5, 119.6, 81.2, 28.7 ppm; MS (API/ES): *m/z*: 442.19 [*M*−1]; found: 442.2.

5-Aminohexahelicene hydrochloride (22): Boc-amino helicene **21** (4.8 g, 10.8 mmol) was stirred overnight in 4 N HCl in dioxane (30 mL) at RT. The resulting solid was collected by filtration, washed with Et_2O, and dried on the rotary evaporator to give HCl salt **22** as a yellow/brown solid. ^{1}H NMR ([D$_6$]DMSO): δ = 8.01–8.14 (m, 7H), 7.92–7.99 (d, 2H), 7.61 (br s, 1H), 7.45–7.52 (dd, 2H), 7.23–7.35 (m, 2H), 6.64–6.75 ppm (m, 2H); ^{13}C NMR ([D$_6$]DMSO): δ = 134.0, 133.4, 132.1, 131.8, 130.9, 130.7, 129.7, 128.8, 128.6, 128.2, 127.7, 127.6, 127.5, 127.1, 126.9, 126.8, 126.4, 125.6, 125.5, 123.5, 122.8 ppm; MS (API/ES): *m/z*: 344.14; found: 344.1.

5-Aminohexahelicene (8): Helicene salt 22 (3.0 g, 6.7 mmol) was suspended in dichloromethane (100 mL) and was washed with saturated $NaHCO_3$ (50 mL). The aqueous layer was extracted with dichloromethane (50 mL) and the combined organic layers were dried over Na_2SO_4 and concentrated to give amine **8** as a brown solid (2.3 g, 85% yield). The material could be further purified by column chromatography over SiO_2 (dichloromethane with 0.5% 7 N NH_3 in EtOH) to provide a yellow–orange material. ^{1}H NMR

([D$_6$]DMSO): $\delta = 8.12$ (d, 1H), 7.93–8.05 (m, 3H), 7.89 (d, 1H), 7.82 (d, 1H), 7.49 (d, 1H), 7.46 (dd, 1H), 7.21 (t, 2H), 7.07 (s, 1H), 6.61–6.69 (dq, 2H), 6.13 ppm (brs, 2H); ^{13}C NMR ([D$_6$]DMSO) $\delta = 144.8$, 136.7, 134.1, 131.9, 131.6, 131.2, 130.1, 128.3, 128.1, 127.7, 127.1, 126.8, 126.0, 125.7, 125.4, 125.1, 124.5, 124.3, 122.7, 120.6, 104.0, 98.1, 91.6 ppm; MS (API/ES): *m/z*: 344.14 [*M*+1]; found: 344.1.

Acknowledgements

The SHG experiments were kindly performed by Prof. G. Coquerel and Arnaud Galland (University of Rouen). The CD measurements were carried out by Prof. Wesley Browne (University of Groningen). We thank Jessica Kerckhoffs and Nicolas Puljic at "Chirality First Time Right", a Syncom daughter operation, for their help during the ligand screening. The analytical department at Syncom BV carried out the analyses and separation of the enantiomers by using chiral preparative HPLC. We are grateful to the European Commission (seventh Framework Program NMP4-SL-2008-214340) for partial funding of this work. We also acknowledge financial support from CONICET of Argentina (PIPs 112-201101-00650 and 112-201101-00594) and the Cesar Milstein Fellowship.

Keywords: cross-coupling · helicenes · optical properties · resolution · scanning tunneling microscopy

[1] E. L. Eliel, S. H. Wilen, L. N. Mander in *Stereochemistry of Organic Compounds*, Wiley-Interscience, New York, **1994**, pp. 1119–1166, p. 1014.
[2] E. Anger, M. Rudolph, L. Norel, S. Zrig, C. Shen, N. Vanthuyne, L. Toupet, J. A. Garreth Williams, C. Roussel, J. Autschbach, J. Crassous, R. Réau, *Chem. Eur. J.* **2011**, *17*, 14178–14198.
[3] T. Balandina, M. W. van der Meijden, O. Ivasenko, D. Cornil, J. Cornil, R. Lazzaroni, R. M. Kellogg, S. De Feyter, *Chem. Commun.* **2013**, *49*, 2207–2209.
[4] M. W. van der Meijden, M. Leeman, E. Gelens, W. L. Noorduin, H. Meekes, W. J. P. van Enckevort, B. Kaptein, E. Vlieg, R. M. Kellogg, *Org. Process Res. Dev.* **2009**, *13*, 1195–1198.
[5] H. Ascolani, M. W. van der Meijden, L. J. Cristina, J. E. Gayone, R. M. Kellogg, J. D. Fuhr, M. Lingenfelder, *Chem. Commun.* **2014**, *50*, 13907–13909.
[6] M. S. Newman, D. Lednicer, *J. Am. Chem. Soc.* **1956**, *78*, 4765–4770.
[7] M. S. Newman, W. B. Lutz, D. Lednicer, *J. Am. Chem. Soc.* **1955**, *77*, 3420–3421.
[8] R. H. Martin, M. Baes, *Tetrahedron* **1975**, *31*, 2135–2137.
[9] H. Wynberg, *Acc. Chem. Res.* **1971**, *4*, 65–73.
[10] a) J. MíŠek, F. Teplý, I. G. Stará, M. Tichý, D. Šaman, I. Císařová, P. VojtíŠek, I. Starý, *Angew. Chem. Int. Ed.* **2008**, *47*, 3188–3191; *Angew. Chem.* **2008**, *120*, 3232–3235; b) F. Teplý, I. G. Stará, I. Starý, A. Kollárovič, D. Šaman, Š. Vyskocil, P. Fiedler, *J. Org. Chem.* **2003**, *68*, 5193–5197.
[11] a) J. Storch, J. Sýkora, J. Čermák, J. Karban, I. Cisarová, A. Růička, *J. Org. Chem.* **2009**, *74*, 3090–3093; b) J. Storch, J. Čermák, J. Karban, I. Cisarová, J. Sýkora, *J. Org. Chem.* **2010**, *75*, 3137–3140.
[12] B. Yang, L. Liu, T. J. Katz, C. A. Liberko, L. L. Miller, *J. Am. Chem. Soc.* **1991**, *113*, 8993–8994.
[13] D. Conreaux, N. Mehanna, C. Herse, J. Lacour, *J. Org. Chem.* **2011**, *76*, 2716–2722.
[14] A. Urbano, *Angew. Chem. Int. Ed.* **2003**, *42*, 3986–3989; *Angew. Chem.* **2003**, *115*, 4116–4119.
[15] Y. Shen, C.-F. Chen, *Chem. Rev.* **2012**, *112*, 1463–1535.
[16] I. Starý, I. G. Stará in *Strained Hydrocarbons*, Wiley-VCH, Weinheim, **2009**, pp. 166–203.
[17] M. Gingras, G. Félix, R. Peresutti, *Chem. Soc. Rev.* **2013**, *42*, 1007–1050.
[18] Z. Yuan Wang, Y. Qi, T. P. Bender, J. Ping Gao, *Macromolecules* **1997**, *30*, 764–769.
[19] G. Pieters, A. Gaucher, D. Prim, J. Marrot, *Chem. Commun.* **2009**, 4827–4828.
[20] A. Perzyna, C. Dal Zotto, J.-O. Durand, M. Granier, M. Smietana, O. Melnyk, I. G. Stará, I. Starý, B. Klepetarova, D. Saman, *Eur. J. Org. Chem.* **2007**, 4032–4037.
[21] R. Pathak, K. Vandayar, W. A. L. van Otterlo, J. P. Michael, M. A. Fernandes, C. B. de Koning, *Org. Biomol. Chem.* **2004**, *2*, 3504–3509.
[22] In the reactions reported by de Koning and co-workers, cyclization was carried out with an alkoxide base with simultaneous irradiation by a high-pressure Hg lamp, with the reaction mixture under N_2 and presumably no O_2, which one might anticipate to be necessary for the dehydrogenation and condensation reactions; furthermore, de Koning and co-workers reported for [5]helicene a doublet at $\delta = 8.56$ ppm for one proton, whereas Fürstner and co-workers[21] report two protons at $\delta = 8.5$ ppm; there are also significant differences between the reported ^{1}H NMR spectra for [4]helicene relative to the data given by Fürstner and co-workers.[21]
[23] V. Mamane, P. Hannen, A. Fürstner, *Chem. Eur. J.* **2004**, *10*, 4556–4575.
[24] C. Wolf in *Dynamic Stereochemistry of Chiral Compounds: Principles and Applications*, Royal Society of Chemistry, Cambridge, **2008**, p. 53.
[25] W. H. Laarhoven, Th. J. H. M. Cuppen, R. F. J. Nivard, *Tetrahedron* **1974**, *30*, 3343–3347.
[26] R. H. Furneaux, V. L. Schramm, P. C. Tyler, *Bioorg. Med. Chem.* **1999**, *7*, 2599–2606.
[27] Boehringer Ingelheim Ltd), WO03007945, **2003**.
[28] R. D. Haworth, *J. Chem. Soc.* **1932**, 1125–1133.
[29] N. Harada, A. Saito, N. Koumura, H. Uda, B. de Lange, W. F. Jager, H. Wynberg, B. L. Feringa, *J. Am. Chem. Soc.* **1997**, *119*, 7241–7248.
[30] A. V. Wiznycia, J. Desper, C. J. Levy, *Chem. Commun.* **2005**, 4693–4695.
[31] K. T. Chapmana, P. L. Durettea, C. G. Caldwella, K. M. Sperowa, L. M. Niedzwieckib, R. K. Harrison, C. Saphos, A. J. Christen, J. M. Olszewski, V. L. Moore, M. MacCoss, W. K. Hagmann, *Bioorg. Med. Chem. Lett.* **1996**, *6*, 803–806.
[32] G. Olah in *Friedel–Craft and Related reactions, vol. II*, Interscience Publishers, New York, **1964**, p. 432.
[33] S. R. Burzynski, L. Musial, U. S. Patent, 6372938, **2002**.
[34] V. Premasagar, V. A. Palaniswamy, E. J. Eisenbraun, *J. Org. Chem.* **1981**, *46*, 2974–2976.
[35] S. D. Walker, T. E. Barder, J. R. Martinelli, S. L. Buchwald, *Angew. Chem. Int. Ed.* **2004**, *43*, 1871–1876; *Angew. Chem.* **2004**, *116*, 1907–1912.
[36] R. Czerwonka, K. R. Reddy, E. Baum, H.-J. Knölker, *Chem. Commun.* **2006**, 711–713.
[37] Schering corporation), WO2008156739, **2008**.
[38] A. Fürstner, V. Mamane, *J. Org. Chem.* **2002**, *67*, 6264–6267.
[39] C. Nevado, A. M. Echavarren, *Chem. Eur. J.* **2005**, *11*, 3155–3164.
[40] E. Soriano, J. Marco-Contelles, *Organometallics* **2006**, *25*, 4542–4553.
[41] W. ten Hoeve, H. Wynberg, *J. Org. Chem.* **1985**, *50*, 4508–4514.
[42] R. M. Kellogg, B. Kaptein, T. R. Vries, *Top. Curr. Chem.* **2007**, *269*, 159–197.
[43] M. S. Newman, R. S. Darlak, L. Tsai, *J. Am. Chem. Soc.* **1967**, *89*, 6191–6193.
[44] G. Levilain, G. Coquerel, *CrystEngComm* **2010**, *12*, 1983–1992.
[45] R. Raval, *Chem. Soc. Rev.* **2009**, *38*, 707–721.
[46] R. Fasel, M. Parschau, K. H. Ernst, *Nature* **2006**, *439*, 449–452.
[47] K.-H. Ernst, S. Baumann, C. P. Lutz, J. Seibel, L. Zoppi, A. J. Heinrich, *Nano Lett.* **2015**, *15*, 5388–5392.
[48] B. S. Green, M. Knossow, *Science* **1981**, *214*, 795–797.
[49] J. Seibel, M. Parschau, K.-H. Ernst, *J. Phys. Chem. C* **2014**, *118*, 29135–29141.

Received: July 16, 2015
Published online on December 14, 2015